

<https://doi.org/10.1038/s43856-025-01242-6>

Cardiovascular measures from abdominal MRI provide insights into abdominal vessel genetic architecture

Check for updates

Nicolas Basty^{1,3}, Elena P. Sorokin^{2,3}, Marjola Thanaj¹, Brandon Whitcher¹, Yi Liu², Jimmy D. Bell¹, E. Louise Thomas^{1,3} & Madeleine Cule^{2,3} ✉

Abstract

Background Cardiovascular disease remains a major source of morbidity and mortality, and population imaging studies have yielded insights into disease etiology and risk.

Methods In this study, we segment the heart, aorta, and vena cava from abdominal magnetic resonance imaging (MRI) scans using deep learning. We generate six image-derived phenotypes (IDP): heart volume, four aortic and one vena cava cross-sectional areas (CSA), from 44,541 UK Biobank participants, and explore their associations with disease outcomes, as well as genetic and environmental factors.

Results Here we show concordance between our IDPs and related IDPs from cardiac magnetic resonance imaging, the current gold standard, and replicate previous findings related to sex differences and age-related changes in heart and vessel dimensions. We identify a significant association between infrarenal descending aorta CSA and incident abdominal aortic aneurysm, and between heart volume and several cardiovascular disorders. In a genome-wide association study, we identify 72 associations at 59 loci (15 novel). We derive a polygenic risk score for each trait and demonstrated an association with thoracic aneurysm diagnosis, pointing to a potential screening opportunity. We demonstrate substantial genetic correlation with cardiovascular traits including aneurysms, varicose veins, dysrhythmia, and cardiac failure. Finally, heritability enrichment analysis implicates vascular tissue in the heritability of these traits.

Conclusions This study illustrates the value of non-specific abdominal MRI for exploring cardiovascular disease risk in cohort studies, and identifies novel genetic associations with vascular dimensions.

Plain language summary

Heart disease is a major health problem. This study explored whether whole-body MRI scans, medical scans that use magnetic fields and radio waves to create detailed images of the inside of the body, could provide useful insights into heart and blood vessel health. Currently MRI is not typically used for heart analysis. By analyzing data from over 44,000 people, we found links between heart size, blood vessel health, and disease risk. We confirmed our results with other types of heart scan and identified inherited (genetic) factors influencing heart and vessel size. Larger aortas were linked to aneurysms (swelling of the artery wall), and heart volume was connected to heart disease. We also developed a genetic risk score that could help predict certain conditions. Our study shows how artificial intelligence (AI) and MRI scans can improve heart disease research and possibly be used to identify and hence prevent heart disease.

Despite its apparently simple structure, the aorta is developmentally complex with substantial regional heterogeneity to “cushion” delicate peripheral tissue from the pulsatile pressure of blood flow¹. Disorders of the vascular system, such as aneurysm and dissection, are a major and preventable cause of death in the developed world^{2,3}.

Recent advancements in implementations of deep learning-based segmentation models for cardiac imaging have demonstrated their potential in accurately quantifying anatomical structures and aiding in disease risk assessment⁴. Studies utilizing cardiac MRI (CMR) have specifically quantified aortic size and highlighted the substantial role of genetic factors in determining the diameter of the ascending

and descending thoracic aorta, as well as their contribution to disease risk^{2,5}.

Distinct genetic factors influence the dimensions of spatially separate ascending aorta regions⁶. Studies of the genetic risk factors for intracranial (IA), thoracic (TAA), and abdominal aortic aneurysms (AAA) identified some shared loci but overall found low genetic correlation between them⁷. Although AAA are more prevalent and have distinct epidemiological risk factors than TAA^{8,9}, and show distinct epidemiological risk factors, quantitative traits capturing the health of abdominal vessels have received relatively less attention than those nearer to the heart. The conventional CMR field of view (FoV) does not cover areas in the lower abdomen; population-level

¹Research Centre for Optimal Health, School of Life Sciences, University of Westminster, London, UK. ²Calico Life Sciences LLC, South San Francisco, CA, USA.

³These authors contributed equally: Nicolas Basty, Elena P. Sorokin, E. Louise Thomas, Madeleine Cule. ✉e-mail: cule@calicolabs.com

assessments of vascular diameter in the abdominal aorta have been infeasible. Given the established differences between the thoracic and abdominal aorta in vessel wall microstructure, developmental origin, and hemodynamic forces^{1,10}, we hypothesize that distinct genetic and epidemiological factors may affect the CSA of the abdominal aorta compared to the thoracic aorta.

We segmented the heart, aorta, and vena cava, from UK Biobank (UKBB) neck-to-knee MRI using deep learning and extracted vessel cross-sectional areas (CSA) both within and outside the CMR FoV, demonstrating the feasibility of extracting cardiovascular features from non-cardiac-specific scans. We find a correlation of greater than 80% with equivalent features derived from CMR in the aortic arch and thoracic descending aorta, regions where there is anatomical overlap (Fig. 1). Our study additionally quantifies the CSA of the infrarenal aorta (most frequent AAA location)⁹, suprarenal aorta, and the vena cava. We also extracted a measure of overall heart volume. We demonstrate that heart volume is associated with dysrhythmia and valve defects and a predictor of major adverse cardiac events (MACE), and that abdominal vessel CSAs are associated with aneurysm and varicose veins.

We explore the contribution of genetic variation to vessel size at different regions and identify shared and non-shared variants, consistent with the distinct developmental origins of different regions of major vessels. We link genetic variation associated with vessel size with regions of the genome close to genes specifically expressed in vascular tissue. Finally, we develop a polygenic risk score (PRS) for vessel CSA and recapitulate our epidemiological findings in a larger cohort.

Methods

Study cohort

The UK Biobank (UKBB) is a population-based cohort of 500,000 participants aged 40–69 years recruited between 2006 and 2010. Starting in 2014, participants were invited to undergo imaging at specialist centers. At the time of the study, abdominal MRI data were available for 44,541 of the participants. The study also collected prospective information on disease outcomes as well as extensive profiling of risk factors, anthropometric measurements, and environmental exposures. Demographics of this cohort are described in Supplementary Data 1. We applied to do research using the UKBB, and permission was granted (Application Number 44584). The UKBB has approval from the North West Multi-Centre Research Ethics Committee (REC reference¹¹:/NW/0382). All measurements were obtained under these ethics, adhering to relevant guidelines and regulations, with written informed consent obtained from all participants.

Image-derived phenotypes

Image processing pipelines for the Dixon MRI and deep learning for image segmentation, are described in ref. 12. Briefly, we trained a convolutional neural network for 3D segmentation using 109 manual expert annotations of the heart, 101 of the aorta and vena cava (Fig. 1A), with training on 80% of the data and testing on 20%. The Dice scores on 20% of out-of-sample testing data were 0.88 (aorta), 0.93 (heart), and 0.82 (vena cava). The aorta was divided into four segments: the ascending aorta, the descending thoracic aorta, the descending suprarenal aorta, and the descending infrarenal aorta. We extracted CSAs via orthogonal planes, removing individuals with CSA >1600 mm² or roundness <0.7 (Supplementary Methods). (Fig. 1B and Supplementary Fig. 1).

Phenome-wide association study

We performed linear (quantitative traits) or logistic (binary traits) regression on the 2425 traits and 890 phecodes with at least 20 cases, adjusting for imaging center, date, scan time, age, sex, BMI, height, and ethnicity (Supplementary Methods).

Survival analysis

Dates of the first occurrence of relevant diseases were defined based on a combination of hospital records, primary care records, self-reports, and death records, and censored at the last recorded follow-up date

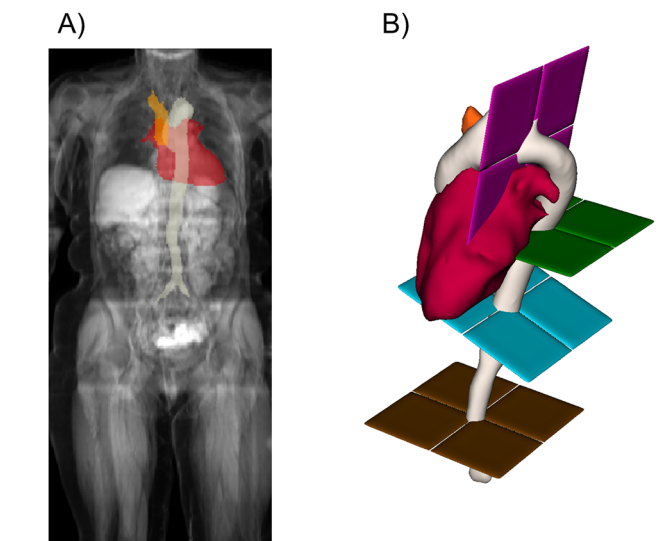


Fig. 1 | Segmentation of abdominal vascular structures from MRI. A Abdominal MRI and segmentations: aorta (white), vena cava (orange), heart (red). Green: Approximate CMR FoV. **B** 3D segmentations: aorta, vena cava, heart, orthogonal planes to extract CSAs: aortic arch (pink), thoracic aorta (green), suprarenal aorta (blue), and infrarenal aorta (brown).

(Supplementary Data 2). Cox proportional hazards models were adjusted for sex, age, weight, and height.

Genetic studies

We performed a genome-wide association study (GWAS) using UKBB imputed genotypes v3, excluding single-nucleotide polymorphisms (SNPs) with minor allele frequency <1% and imputation quality <0.9 using BOLT-LMM¹³ (Supplementary Methods). We verified that the test statistics showed no overall inflation compared to the expectation by examining the intercept of linkage disequilibrium score regression (LDSC)¹⁴ (Supplementary Data 3). To identify potential causal variants, we performed approximate conditional analysis using GCTA¹⁵, considering all variants that passed quality control measures and were within 500 kb of a locus index variant (Supplementary Methods). We estimated the heritability of each trait using restricted maximum likelihood as implemented in BOLT v2.3.2¹⁶ To identify relevant tissues and cell types contributing to IDP heritability, we used stratified LDSC^{17,18} to examine enrichment in regions of the genome containing genes specific to particular tissues or cell types.

We downloaded summary statistics for 32 relevant traits, including CMR IDPs, disease outcomes identified as correlated with our IDPs, and other cardiovascular health measures (Supplementary Data 4). To identify potentially causal genes at each locus, we downloaded QTL data from GTEx (phs000424.v7.p2) to seek evidence for colocalisation with expression in one of five cardiovascular tissues.

Rare variant association study

After quality control and variant annotation (Supplementary Methods), we performed rare variant burden and SKAT testing as implemented in SAIGE-GENE¹⁹, using a mixed-effects model.

Polygenic risk score calculation

We trained PRS using pruning and thresholding ($R^2 = 0.1$ and a range of p values: $1e-8$ to 0.1) in a set of UKBB individuals ($n = 2567$) not included in GWAS. We then calculated scores in a non-imaging European ancestry cohort with complete covariates ($n = 250,753$) using the optimal p value threshold.

Survival modeling with PRS

We associated standardized PRS with time-to-event data in participants of European ancestry who were not in the imaging subcohort for aortic aneurysm, myocardial infarction, and stroke, taking the first recorded event as survival time. Since PRS is conferred at birth, we considered the entire patient history as the follow-up period. Cox proportional hazard models were adjusted for other factors conferred at birth, genetic sex, and the first ten principal components of genetic ancestry.

Statistics and reproducibility

This study is exploratory, and therefore, the sample size was not pre-determined. No replication was performed.

Reporting summary

Further information on research design is available in the Nature Portfolio Reporting Summary linked to this article.

Results

Population-scale inference of abdominal cardiovascular IDPs

We extracted heart volume and aortic arch, descending aorta (thoracic, suprarenal, and infrarenal), and vena cava CSAs from 44,451 individuals (Fig. 1). On average, men had higher values than women for all IDPs (Fig. 2A and Supplementary Data 5, 6). After adjusting for sex, imaging center, scan date, and scan time, CSAs were positively associated with age (Fig. 2B and Supplementary Data 7).

We computed the correlation between abdominal and CMR IDPs in the same cohort¹¹. In the aorta, the strongest correlation was between the CMR descending aorta and the abdominal thoracic descending aorta, with a progressively weaker correlation further down the aorta (Fig. 2C). This provides evidence that quantitative traits extracted from abdominal MRI capture variation between individuals, making this the first population-scale survey of vessel size outside of the cardiac region. Heart volume was positively correlated with atrial and ventricular volumes and diameters of the ascending and descending thoracic aorta, and negatively correlated with ventricular ejection fractions.

Phenome-wide association study links vascular IDPs with cardiovascular disease outcomes and quantitative traits

To understand whether these IDPs are associated with disease outcomes, and how these associations varied along the length of the abdominal aorta, we conducted a disease phenome-wide association study with two stages. First, to maximize power to detect associations across a broad range of outcomes, we performed a phenome-wide association study based on disease labels extracted from hospital records, without considering the timing of the event relative to the scan date. We found an association between aortic arch CSA and hypertension, between the suprarenal aorta and vena cava CSA and varicose veins, and between infrarenal aorta CSA and aneurysms. Type 2 diabetes (T2D) was associated with lower heart volume and smaller vessel CSA, with heart volume additionally associated with cardiomyopathy, valve disorders, heart failure, angina, and dysrhythmias (Fig. 3A and Supplementary Data 8). In a phenome-wide association study across a broader range of quantitative traits, vessel CSA was additionally associated with physical activity, blood pressure, age, and body size, and with alcohol consumption (Supplementary Figs. 2–6 and Supplementary Data 9). Among cardiovascular disease-relevant biomarkers, triglycerides were most strongly associated with vessel CSA. In the second stage, we assessed whether the region-specific IDPs had predictive value for three composite cardiovascular disease outcomes identified as significantly associated with cardiovascular IDPs in the initial phenome-wide scan. Infrarenal aorta CSA was a risk factor for incident aneurysm, while increased heart volume was a risk factor for MACE (Fig. 3B). No other IDPs were significantly associated with incident disease after adjustment for multiple testing, although due to the relatively short follow-up period (median 3.5 years, range 1.8–7.7 years) from the imaging visit, power to detect associations is limited by the small number of events.

Given the direct relationship between vessel CSA and aneurysm, and the existing evidence for distinct risk factors for aneurysm in different anatomical locations, we refined our analysis of incident aneurysm by fitting a separate multivariate model for incident AAA, TAA, and small vessel IA. Infrarenal aorta CSA was associated with risk of AAA, suggesting that this measure was specific to this outcome, while heart volume was additionally associated with risk of TAA and no CSAs were associated with IA (Supplementary Fig. 7).

Finally, to estimate the prevalence of undiagnosed enlargement of the abdominal aorta, we used the most commonly used definition of infrarenal descending aorta CSA >700 mm² (3 cm diameter) to characterize AAA⁹ in the UKBB cohort. We identified 126 men and seven women meeting the criteria for AAA. Of these, only nine men (7%) and one woman (14%) had a diagnosis of AAA in the available medical record, pointing to substantial underdiagnosis of this condition (Fig. 3C and Supplementary Data 10). Surprisingly, only 20% of men and 17% of women with a diagnosis of AAA exceeded this threshold at the time of imaging, which may reflect treatment, timing of scanning relative to diagnosis, or aneurysm affecting a different region of the abdominal aorta.

Although aneurysm diagnosis is more common in men than in women, outcomes in women are considerably worse^{20,21}. This has been attributed to the cardioprotective effects of estrogen or other hormones, supported with evidence from epidemiological studies²² and animal models^{23,24}. An alternative possible contributing factor is that using a single threshold does not adequately capture women at risk^{25,26}. The 3 cm threshold at infrarenal descending aorta is the 99.35th percentile for men in our dataset, which for women would correspond to a diameter of 2.6 cm. Future studies could explore whether identification of women at risk with a sex-specific threshold increases diagnoses and improves outcomes.

Genome-wide association study identifies 59 loci associated with cardiovascular IDPs

Motivated by the heterogeneity in association with disease risk described above, we conducted a separate GWAS for each trait, with three goals: to characterize variants associated with each IDP, to identify candidate genes and tissues associated with these traits, and to develop a PRS to explore the larger non-imaging cohort. SNP heritability of vessel CSAs ranged from 17–42%, with heritability of the heart volume estimated to be 45% (Supplementary Data 11 and Supplementary Fig. 8), confirming that vascular IDPs have a substantial heritable component. The heritability did not differ significantly between sexes (Supplementary Fig. 9).

We identified a total of 59 loci associated with at least one trait at genome-wide significance ($p < 5e-8$) (Fig. 4A, Supplementary Data 12, and Supplementary Fig. 10), seven of which were associated with multiple traits. 44/72 trait-locus pairs reached a more stringent study-wide threshold ($p < 8e-9$). Except at the *PLCE1* locus, where there were two independent signals (Supplementary Data 13), colocalisation revealed that where two traits are associated at the same locus, they likely share the same lead SNP. The correlation in effect sizes between sexes was 0.94 (Supplementary Fig. 11).

We found a genetic correlation between aortic aneurysm and vessel CSA (especially suprarenal aorta, $r_g = 0.87$), and between varicose veins and vessel CSA (especially vena cava, $r_g = 0.37$). There was little genetic correlation between vessel CSA and other cardiovascular traits such as pulse pressure, ischemic heart disease, and coronary artery disease (Fig. 4B, C and Supplementary Figs. 14, 15), although several loci have been implicated in previous studies of cardiovascular traits and outcomes (Supplementary Fig. 14). Using stratified LDSC¹⁷, we identified enrichment in cardiovascular cell types including aorta and fetal heart for all of the traits except vena cava CSA (Fig. 5A and Supplementary Fig. 12).

Of the 72 trait-locus pairs, 47 show evidence (posterior probability >0.9) of a shared signal with at least one CMR IDP (Supplementary Fig. 13). In particular, 20 of the 26 genome-wide-significant loci associated with the thoracic descending aorta were previously reported in a study of CMR-derived descending aorta³, and 12 and nine heart volume loci were reported in left ventricular end systolic volume and left ventricular stroke volume,

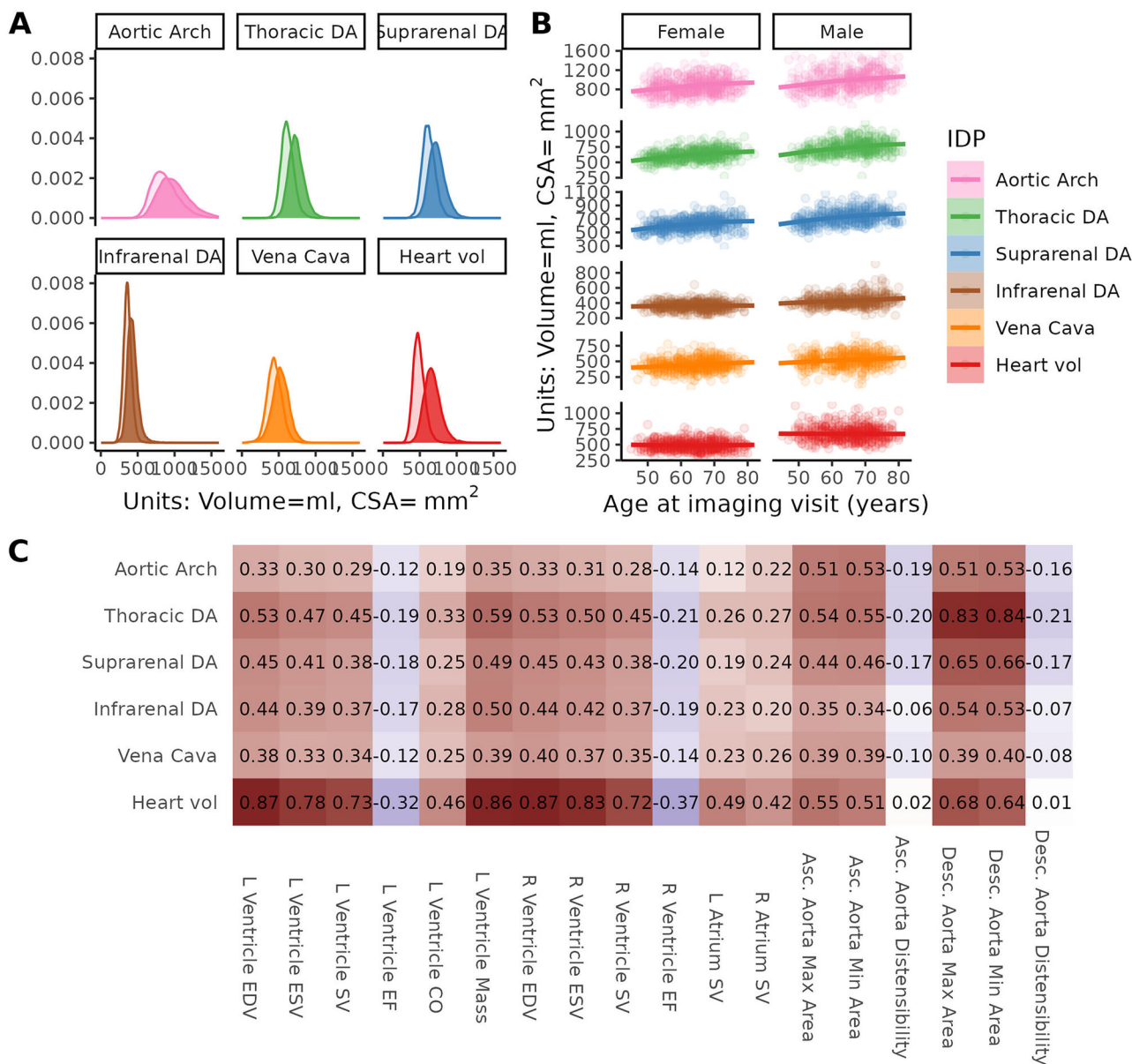


Fig. 2 | Summary of IDPs. A IPD distributions: volume (heart), CSAs (thoracic, suprarenal, and infrarenal descending aorta, aortic arch, and vena cava). Women: transparent, Men: solid. B IDP relationships with age and sex. C Pearson correlation

between abdominal IDPs and CMR IDPs¹¹. DA descending aorta, EDV end diastolic volume, ESV end systolic volume, SV stroke volume, EF ejection fraction, CO cardiac output.

respectively (Supplementary Fig. 13)²⁷. CMR-based descending aorta diameter is genetically correlated ($r_g = 0.91$) with thoracic descending aorta CSA, and a weaker correlation with CSA measures lower in the abdomen (Fig. 4C); ascending aorta diameter has the strongest genetic correlation with aortic arch CSA ($r_g = 0.77$). Heart volume from abdominal MRI is genetically correlated with left ventricular end systolic and diastolic volume and with stroke volume, and negatively genetically correlated with left ventricular ejection fraction.

In an exome-wide association study, an association was observed between rare loss-of-function variants in *WNT10B* and decreased heart volume ($p = 1.0e-7$) (Supplementary Fig. 16). *WNT10B*, a canonical WNT ligand, is expressed within intercalated disks surrounding cardiomyocytes in the human heart²⁸. In mice, cardiac injury increases *WNT10B* expression, and a gain-of-function in this gene improves ventricular recovery versus wild-type, by stimulating angiogenesis, large vessel formation, and cardiomyogenesis²⁸. In addition to rebuilding heart tissue after injury, our observation suggests that *WNT10B* functions in the developmental regulation of heart size.

We identified 31 genes with evidence (posterior probability >0.7) of colocalization of an eQTL in at least one vascular tissue with at least one IDP, with several showing evidence for association in multiple tissues or with multiple IDPs (Fig. 5B and Supplementary Data 14). For example, a locus overlapping *LRP1* and *STAT6* is associated with the suprarenal aorta and thoracic descending aorta CSA. Both signals localise with changes in *LRP1* expression in both tibial and aortic arteries. *LRP1* is an endocytic and signaling receptor with an established role in protection from aneurysms²⁹, and variants at this locus have been associated with acute aortic dissection³⁰.

In the infrarenal descending aorta, we identified region-specific associations at the *WNT7A*, *FUK*, and *MRC2* loci. A novel signal near *MRC2* associated specifically with infrarenal aorta CSA colocalizes with expression of *MRC2* in aortic and tibial artery. The expression- and CSA-increasing allele is in linkage disequilibrium with a variant that has been associated with increased risk of AAA in a recent multi-ancestry GWAS³⁰. *MRC2* (mannose receptor, C type 2) is a cell surface receptor that mediates intracellular degradation of collagen, and low levels have been implicated in fibrosis³¹,

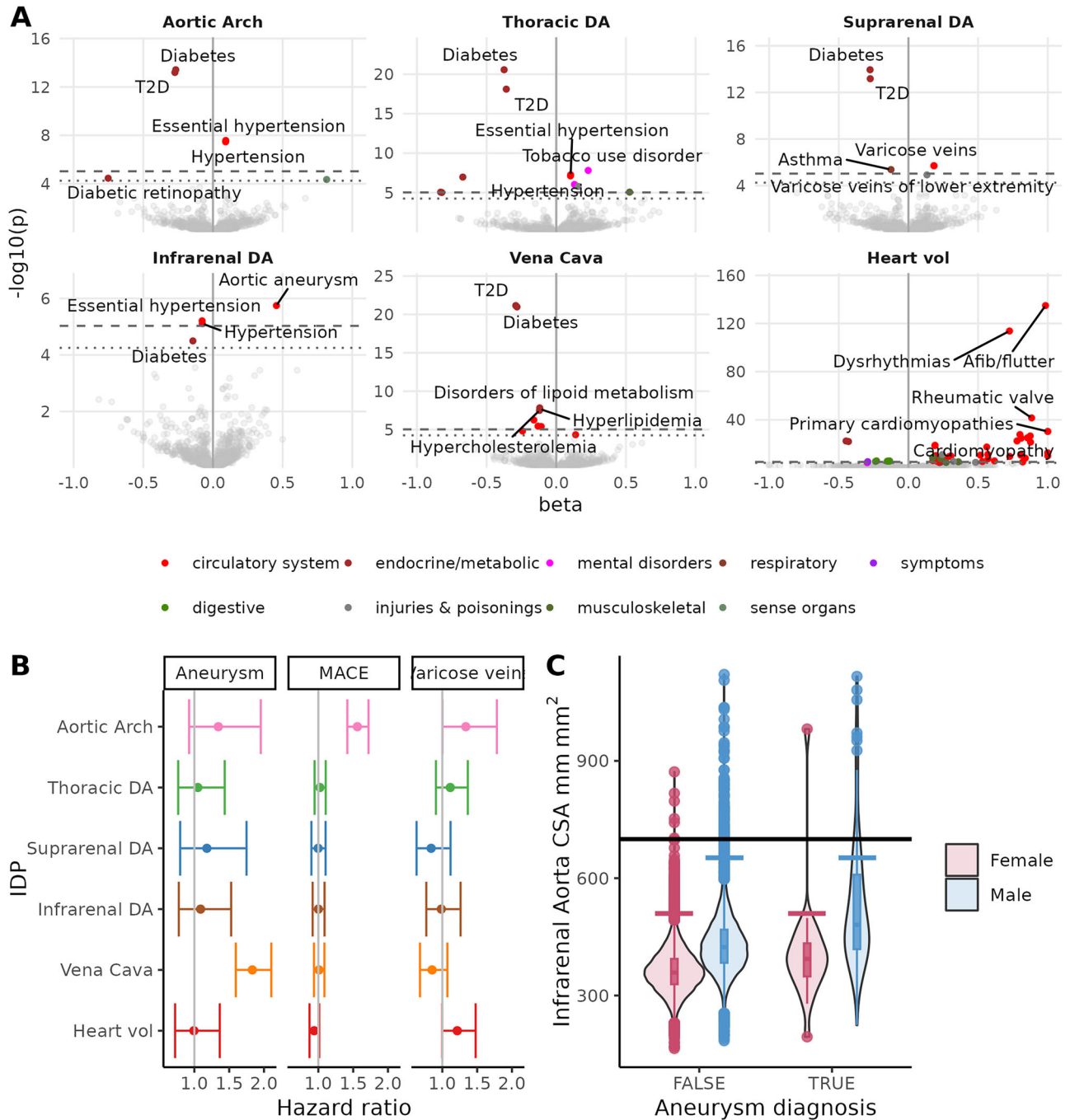


Fig. 3 | Disease associations with abdominal IDPs. A Disease phenome associations between IDPs and disease PheCodes are defined based on hospitalization records. T2D type 2 diabetes. X-axis limited to [-1, 1] and y-axis limited to a maximum *p* value of 10e-50. **B** Log hazard ratio for three combined outcomes:

Aneurysm, MACE, and Varicose veins. Vertical bars as in (B). **C** Infrarenal aorta CSA by AAA diagnosis status and sex. Black horizontal line: literature suggested threshold for infrarenal aortic aneurysm.

aging-related dysregulation of extracellular matrix dynamics³², and aortic root aneurysm in patients with Marfan syndrome³³.

Polygenic risk scores for aortic vessel IDPs are predictive of time-to-event for aneurysm diagnoses

The PRS derived for each IDP trait explained between 5 and 14% of their respective phenotypic variance, with higher percentages for the aortic vessel IDPs (Supplementary Data 15). Using 250,753 European ancestry individuals in the UKBB without imaging data, we assessed associations of PRS across the medical phenome. PRS for all four aorta traits were associated with cardiovascular diagnoses, including thoracic descending aorta PRS and

aneurysms, cardiac dysrhythmias, and hypertension (Supplementary Fig. 17 and Supplementary Data 16). Furthermore, thoracic descending aorta PRS was associated with time to first aortic aneurysm diagnosis (FDR <0.05) (Supplementary Data 17 and Supplementary Fig. 18).

To assess the contribution of the PRS of each anatomical location to the risk of aneurysm at distinct locations, we fitted multi-PRS models to AAA, TAA, and IA. In these models, thoracic aortic CSA PRS was associated with incident TAA. This contrasts with the phenotypic association (Fig. 3), which identified infrarenal CSA as predictive of AAA. This may reflect the relatively higher prevalence of AAA, together with the higher heritability of thoracic aorta CSA.

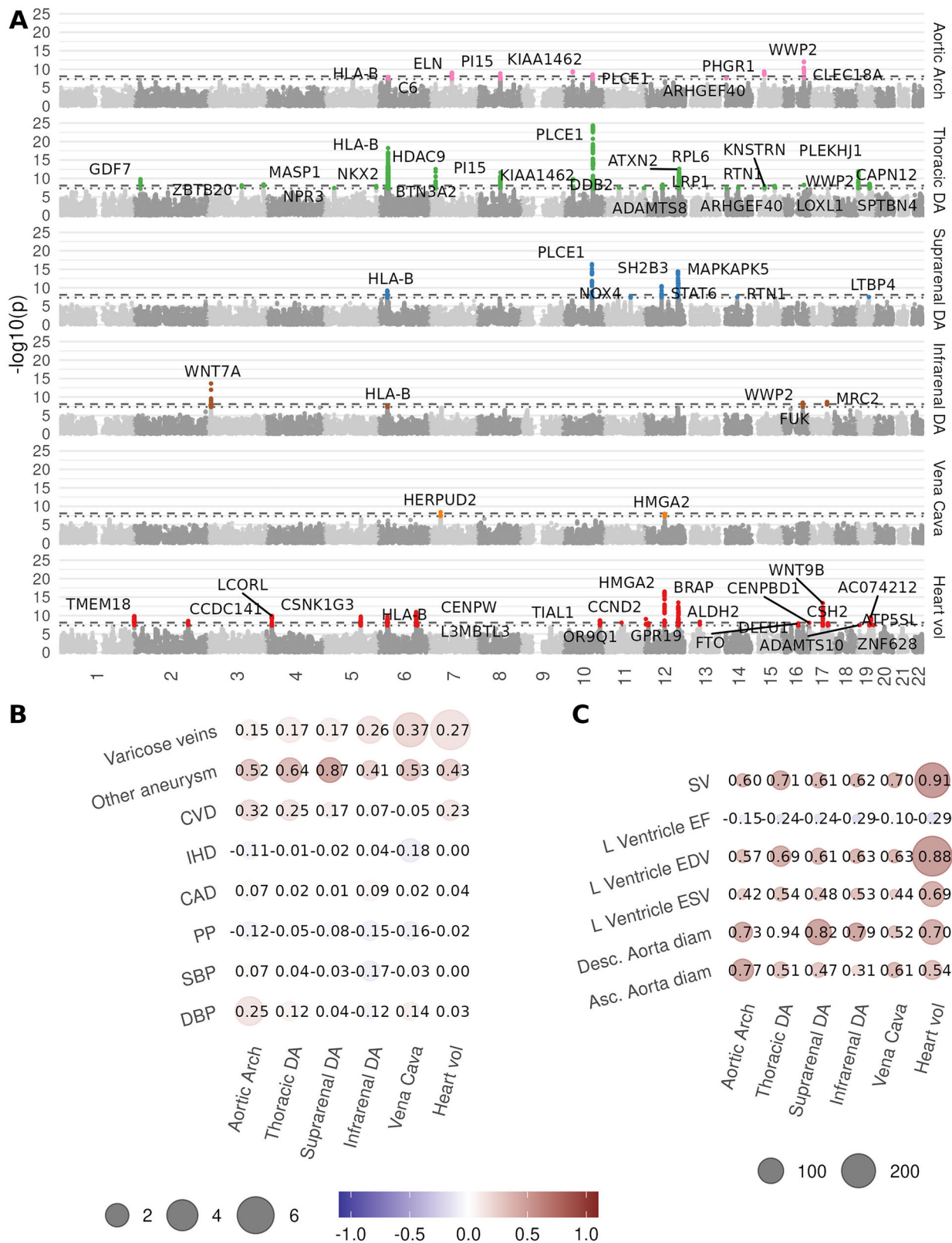


Fig. 4 | Genetic associations with abdominal IDPs. A Manhattan plot. Dotted line: single-trait significance threshold (5e-8). Dashed line: study-wide significance threshold (8e-9). Loci reaching study-wide significant locus is labeled with the closest gene. **B** Genetic correlation between IDPs and cardiovascular complex traits. CAD coronary artery disease, PP pulse pressure, SBP systolic blood pressure, DBP

diastolic blood pressure. Point sizes are $-\log_{10}(p)$ of the genetic correlation. Color is a genetic correlation. **C** Genetic correlation between IDPs and measures derived from CMR. SV stroke volume, ESV end systolic volume, EF ejection fraction, EDV end diastolic volume.

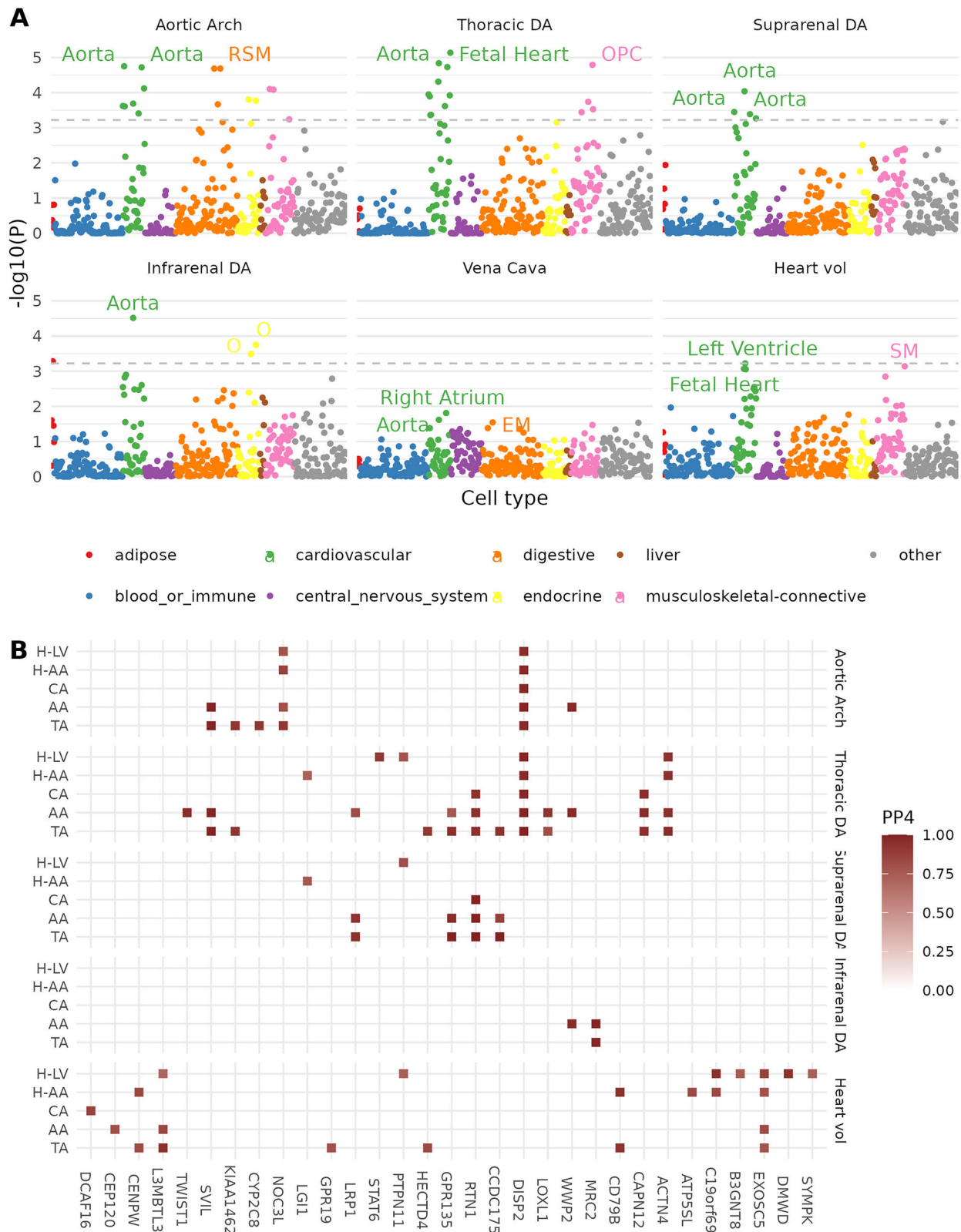


Fig. 5 | Heritability enrichment and colocalization with gene expression.
A Heritability enrichment. Dashed horizontal line at FDR of 0.05. Y-axis: P value of the coefficient of the annotated tissue in a model adjusting for baseline genome features. The top three tissue/cell types are labeled for each IDP. EM esophagus muscularis, O ovary, OPC osteoblast primary cells, SM skeletal muscle.

B Colocalisation probabilities associated with changes in gene expression in cardiovascular tissues. H-LV heart left ventricle, H-AA heart atrial appendage, CA coronary artery, AA aortic artery, TA tibial artery. Colocalisations with $PP4 > 0.7$ are colored.

Discussion

In this study, we used deep learning to extract cardiovascular IDPs from abdominal MRI in a cohort of 44,541 UKBB participants, providing population reference ranges for the diameter of blood vessels in the lower abdomen. We demonstrated that, where there was anatomical overlap, these measures were concordant with those from CMR.

In a phenome-wide association study, larger heart volume was associated with cardiomyopathy, valve disorders, heart failure, angina, and dysrhythmias. Lower heart volume was associated with T2D, consistent with a recent study using CT-based whole heart volume, which found that smaller volumes were more common in individuals with diabetes³⁴. T2D has been associated with increased left ventricular mass³⁵, perhaps reflecting the increased prevalence of obesity in T2D patients³⁶. These seemingly contradictory results may be explained by differences in methodological approaches, or in heterogeneity in the etiology of different cardiovascular disease outcomes, with smaller volumes associated with non-obstructive coronary artery disease (CAD) and larger volumes associated with obstructive CAD³⁴. Indeed, we found larger heart volume to be associated with physical activity and other self-reported health indicators. Taken together, this indicates that larger heart volumes can reflect either cardiovascular health (lower risk of metabolic disease, lower heart rate, higher self-reported health satisfaction) or increased cardiovascular risk (higher risk of atrial fibrillation, rheumatic heart disease, or cardiomyopathy), with more precise measurements needed to distinguish between these factors. In addition, smaller vessel CSAs are associated with T2D, thought to be a factor in the reduced incidence of aneurysms in people with T2D^{37,38}.

We found a significant association between the infrarenal aorta and AAA in a time-to-event model³⁹. This demonstrates the value of making measurements at multiple locations. Longitudinal measurements and relevant outcome data will be required to evaluate whether aortic diameter alone is a clinically useful measure in screening for aneurysm risk, and to potentially define more clinically useful sex-specific thresholds.

While our measurements identified fewer genome-wide significant loci than recent studies based on CMR IDPs, likely due to the lower precision of our measurements, by expanding the FoV to include the infrarenal aortic region, we gain new insight into the genetic architecture of abdominal aorta structure at different anatomical locations, as well as potential risk factors for AAA. Of particular interest, an eQTL analysis implicated *MRC2* as a potential causal gene specifically associated with infrarenal aorta CSA, consistent with the relative importance of collagen and elastin content in the abdominal and thoracic aorta¹⁰. This highlights the value of quantitative measures across a larger anatomical region and suggests that larger sample sizes will lead to better characterization of risk factors for AAA and other vascular disorders.

Finally, this study points to the untapped screening potential of routinely acquired medical images. Repurposing images that are routinely collected for clinical investigations to detect aortic enlargements may provide a useful adjunct to ongoing screening programmes and a valuable tool in the majority of countries where screening is not possible. Furthermore, we suggest that a single threshold for AAA detection in women could partly account for the paradoxical observation that aneurysms are less frequently observed, but more serious, in women. Evaluation of the clinical utility and impact of routine scan screening and sex-specific thresholds will require future prospective studies.

This study has some limitations. The images used in this study have lower resolution than the CMR protocol used by UKBB, and are not optimized to image flowing blood and the beating heart. Therefore, we are unable to measure wall thickness or distensibility of the abdominal aorta. Heart volume measurements are noisy as they depend on where the segmentation places the boundary between the heart and the incoming and outgoing vessels, a consequence of the acquisition covering 17 s and not accounting for cardiac motion. Despite these image acquisition-related drawbacks, we found phenotypic and genetic correlation between CMR and abdominal IDPs.

The UKBB imaging cohort is “healthier” than the wider UK population⁴⁰, predominantly white, and only includes participants older than 40. This study has a 3-year follow-up period since the imaging visit, limiting the power of time-to-event studies. In addition, we do not have access to some potentially important information, such as medication compliance and effectiveness of blood pressure or glycemic control, which are known to influence cardiovascular outcomes. We were unable to study the impact of some known collagen or valve disorders due to their low prevalence in the study population (Supplementary Data 18). In our genetic study, which has a longer follow-up since the risk is present from birth, data prior to the widespread adoption of electronic medical records in 1997 is less complete, relying for this period on self-reported data.

Data availability

Quantitative traits will be returned to the UK Biobank and will be made available to qualified researchers (<https://www.ukbiobank.ac.uk>). GWAS summary statistics will be made available upon publication under accession numbers GCST90568442–GCST90568447 via the NHGRI-EBI GWAS catalog (<https://www.ebi.ac.uk/gwas/>).

Code availability

Code to generate the segmentations is based on <https://github.com/calico/ukbb-mri-sseg>. Additional code to generate the cross-sectional areas will be made available upon request.

Received: 15 September 2023; Accepted: 4 November 2025;

Published online: 02 February 2026

References

- Ohyama, Y., Redheuil, A., Kachenoura, N., Ambale Venkatesh, B. & Lima, J. A. C. Imaging insights on the aorta in aging. *Circ. Cardiovasc. Imaging* **11**, e005617 (2018).
- Tcheandjieu, C. et al. High heritability of ascending aortic diameter and trans-ancestry prediction of thoracic aortic disease. *Nat. Genet.* **54**, 772–782 (2022).
- Pirruccello, J. P. et al. Deep learning enables genetic analysis of the human thoracic aorta. *Nat. Genet.* **54**, 40–51 (2021).
- Chen, C. et al. Deep learning for cardiac image segmentation: a review. *Front. Cardiovasc. Med.* **7**, 25 (2020).
- Benjamins, J. W. et al. Genomic insights in ascending aortic size and distensibility. *EBioMedicine* **75**, 103783 (2022).
- Nekoui, M. et al. Spatially distinct genetic determinants of aortic dimensions influence risks of aneurysm and stenosis. *J. Am. Coll. Cardiol.* **80**, 486–497 (2022).
- van't Hof, F. N. G. et al. Shared genetic risk factors of intracranial, abdominal, and thoracic aneurysms. *J. Am. Heart Assoc.* <https://doi.org/10.1161/JAHA.115.002603> (2016).
- Shaw, P. M., Loree, J., Gibbons, R. C. & McCoy, T. M. Abdominal Aortic Aneurysm (Nursing). In *StatPearls* (StatPearls Publishing, 2022).
- Wang, L. J., Prabhakar, A. M. & Kwolek, C. J. Current status of the treatment of infrarenal abdominal aortic aneurysms. *Cardiovasc. Diagn. Ther.* **8**, S191–S199 (2018).
- Tsamis, A., Krawiec, J. T. & Vorp, D. A. Elastin and collagen fibre microstructure of the human aorta in ageing and disease: a review. *J. R. Soc. Interface* **10**, 20121004 (2013).
- Bai, W. et al. A population-based phenome-wide association study of cardiac and aortic structure and function. *Nat. Med.* **26**, 1654–1662 (2020).
- Liu, Y. et al. Genetic architecture of 11 organ traits derived from abdominal MRI using deep learning. *Elife* <https://doi.org/10.7554/eLife.65554> (2021).
- Loh, P. R. et al. Efficient Bayesian mixed-model analysis increases association power in large cohorts. *Nat. Genet.* **47**, 284–290 (2015).

14. Bulik-Sullivan, B. K. et al. LD score regression distinguishes confounding from polygenicity in genome-wide association studies. *Nat. Genet.* **47**, 291–295 (2015).
15. Yang, J. et al. Conditional and joint multiple-SNP analysis of GWAS summary statistics identifies additional variants influencing complex traits. *Nat. Genet.* **44**, 369–375 (2012).
16. Loh, P. R., Kichaev, G., Gazal, S., Schoech, A. P. & Price, A. L. Mixed-model association for biobank-scale datasets. *Nat. Genet.* **50**, 906–908 (2018).
17. Finucane, H. K. et al. Heritability enrichment of specifically expressed genes identifies disease-relevant tissues and cell types. *Nat. Genet.* **50**, 621–629 (2018).
18. Finucane, H. K. et al. Partitioning heritability by functional annotation using genome-wide association summary statistics. *Nat. Genet.* **47**, 1228–1235 (2015).
19. Zhou, W. et al. Scalable generalized linear mixed model for region-based association tests in large biobanks and cohorts. *Nat. Genet.* **52**, 634–639 (2020).
20. Blanchard, J. F. Epidemiology of abdominal aortic aneurysms. *Epidemiol. Rev.* **21**, 207–221 (1999).
21. Norman, P. E. & Powell, J. T. Abdominal aortic aneurysm. *Circulation* **115**, 2865–2869 (2007).
22. Villard, C. et al. Differential expression of sex hormone receptors in abdominal aortic aneurysms. *Maturitas.* **96**, 39–44 (2017).
23. Wu, X. -F. et al. The role of estrogen in the formation of experimental abdominal aortic aneurysm. *Am. J. Surg.* **197**, 49–54 (2009).
24. Ailawadi, G. et al. Gender differences in experimental aortic aneurysm formation. *Arterioscler. Thromb. Vasc. Biol.* **24**, 2116–2122 (2004).
25. Forbes, T. L., Lawlor, D. K., DeRose, G. & Harris, K. A. Gender differences in relative dilatation of abdominal aortic aneurysms. *Ann. Vasc. Surg.* **20**, 564–568 (2006).
26. Brown, P. M., Zelt, D. T. & Sobolev, B. The risk of rupture in untreated aneurysms: the impact of size, gender, and expansion rate. *J. Vasc. Surg.* **37**, 280–284 (2003).
27. Pirruccello, J. P. et al. Analysis of cardiac magnetic resonance imaging in 36,000 individuals yields genetic insights into dilated cardiomyopathy. *Nat. Commun.* **11**, 2254 (2020).
28. Paik, D. T. et al. Wnt10b gain-of-function improves cardiac repair by arteriole formation and attenuation of fibrosis. *Circ. Res.* **117**, 804–816 (2015).
29. Strickland, D. K., Au, D. T., Cunfer, P. & Muratoglu, S. C. Low-density lipoprotein receptor-related protein-1: role in the regulation of vascular integrity. *Arterioscler. Thromb. Vasc. Biol.* **34**, 487–498 (2014).
30. Roychowdhury, T. et al. Genome-wide association meta-analysis identifies risk loci for abdominal aortic aneurysm and highlights PCSK9 as a therapeutic target. *Nat. Genet.* **55**, 1831–1842 (2023).
31. López-Guisa, J. M. et al. Mannose receptor 2 attenuates renal fibrosis. *J. Am. Soc. Nephrol.* **23**, 236–251 (2012).
32. Podolsky, M. J. et al. Age-dependent regulation of cell-mediated collagen turnover. *JCI Insight* <https://doi.org/10.1172/jci.insight.137519> (2020).
33. Iosef, C. et al. Quantitative proteomics reveal lineage-specific protein profiles in iPSC-derived Marfan syndrome smooth muscle cells. *Sci. Rep.* **10**, 20392 (2020).
34. Foldyna, B. et al. Small whole heart volume predicts cardiovascular events in patients with stable chest pain: insights from the PROMISE trial. *Eur. Radiol.* **31**, 6200–6210 (2021).
35. Santra, S. et al. Comparison of left ventricular mass in normotensive type 2 diabetes mellitus patients with that in the nondiabetic population. *J. Cardiovasc. Dis. Res.* **2**, 50–56 (2011).
36. Eguchi, K. et al. Association between diabetes mellitus and left ventricular hypertrophy in a multiethnic population. *Am. J. Cardiol.* **101**, 1787–1791 (2008).
37. Raffort, J. et al. Diabetes and aortic aneurysm: current state of the art. *Cardiovasc Res.* **114**, 1702–1713 (2018).
38. Shah, A. D. et al. Type 2 diabetes and incidence of cardiovascular diseases: a cohort study in 1.9 million people. *Lancet Diab. Endocrinol.* **3**, 105–113 (2015).
39. Solberg, S., Forsdahl, S. H., Singh, K. & Jacobsen, B. K. Diameter of the infrarenal aorta as a risk factor for abdominal aortic aneurysm: the Tromsø Study, 1994–2001. *Eur. J. Vasc. Endovasc. Surg.* **39**, 280–284 (2010).
40. Lyall, D. M. et al. Quantifying bias in psychological and physical health in the UK Biobank imaging sub-sample. *Brain Commun.* **4**, fcac119 (2022).

Acknowledgements

This research was conducted using the UKBB Resource under Application Number 44584 and was funded by Calico Life Sciences LLC. We thank Kevin Wright and Nick van Bruggen for their feedback on the manuscript.

Author contributions

N.B., E.P.S., J.D.B., and E.L.T. designed the study. N.B., B.W., and Y.L. implemented the image processing methods. M.T. defined the disease and physiological condition categories. M.C. performed the data processing. E.P.S. performed genetic analyses. N.B., E.L.T., E.P.S., and M.C. drafted the manuscript. All authors edited, read, and approved the manuscript.

Competing interests

E.P.S. and M.C. are employees and Y.L. a former employee of Calico Life Sciences LLC. The remaining authors declare no competing interests.

Additional information

Supplementary information The online version contains supplementary material available at <https://doi.org/10.1038/s43856-025-01242-6>.

Correspondence and requests for materials should be addressed to Madeleine Cule.

Peer review information *Communications Medicine* thanks Lilia M. Sierra-Galan and the other, anonymous, reviewer(s) for their contribution to the peer review of this work.

Reprints and permissions information is available at <http://www.nature.com/reprints>

Publisher's note Springer Nature remains neutral with regard to jurisdictional claims in published maps and institutional affiliations.

Open Access This article is licensed under a Creative Commons Attribution-NonCommercial-NoDerivatives 4.0 International License, which permits any non-commercial use, sharing, distribution and reproduction in any medium or format, as long as you give appropriate credit to the original author(s) and the source, provide a link to the Creative Commons licence, and indicate if you modified the licensed material. You do not have permission under this licence to share adapted material derived from this article or parts of it. The images or other third party material in this article are included in the article's Creative Commons licence, unless indicated otherwise in a credit line to the material. If material is not included in the article's Creative Commons licence and your intended use is not permitted by statutory regulation or exceeds the permitted use, you will need to obtain permission directly from the copyright holder. To view a copy of this licence, visit <http://creativecommons.org/licenses/by-nc-nd/4.0/>.

© The Author(s) 2026